Semiconducting Oxides to Facilitate the Conversion of Solar Energy to Chemical Fuels

ARTICLE *in* JOURNAL OF PHYSICAL CHEMISTRY LETTERS · SEPTEMBER 2010

Impact Factor: 7.46 · DOI: 10.1021/jz100961d

4 AUTHORS, INCLUDING:

Andriy Palasyuk
Iowa State University
29 PUBLICATIONS **224** CITATIONS
SEE PROFILE

Paul A. Maggard
North Carolina State University
108 PUBLICATIONS **1,724** CITATIONS
SEE PROFILE

THE JOURNAL OF PHYSICAL CHEMISTRY Letters

PERSPECTIVE

pubs.acs.org/JPCL

Semiconducting Oxides to Facilitate the Conversion of Solar Energy to Chemical Fuels

Upendra A. Joshi, Andriy Palasyuk, David Arney, and Paul A. Maggard*

Department of Chemistry, North Carolina State University, Raleigh, North Carolina 27695-8204.

ABSTRACT The rising significance of producing useful chemical fuels from sunlight has motivated an upsurge of photochemical research, as shown by the growing diversity of chromophores, redox catalysts, and reactivity studies. However, their synergistic integration within artificial photosynthetic systems requires shareable platforms. Early transition-metal oxides have exhibited effective chromophoric/electronic properties across many systems, which has enabled outstanding photocatalytic water splitting efficiencies, but only under ultraviolet irradiation. Semiconducting modifications of these oxides have been investigated that both extend their absorption deep into the visible region and also closely bracket the redox potentials for water splitting and carbon dioxide reduction. Their coupling to surface-anchored molecular catalysts in order to lower kinetic barriers and provide product selectivity is anticipated to lead to studies involving the dynamic interplay of photons, charge carriers, and catalyst turnover.

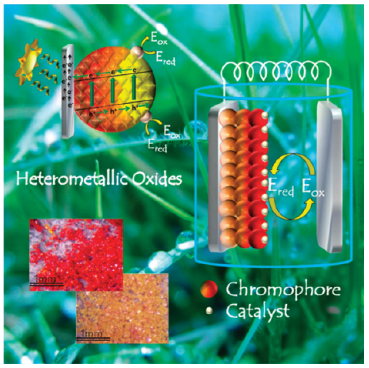

Photochemical investigations for the production of useful chemical fuels currently cover a wide range of important reactions, such as water splitting to generate hydrogen,[1] the reduction of carbon dioxide,[2] as well as efforts in environmental remediation.[3] Research strategies in this field are delineated by the plethora of choices for light-harvesting chromophores and molecular catalysts, varied routes to the hierarchical assembly and multicomponent cooperativity of their chemical and electronic architectures, and also more application-relevant parameters such as stability, cost, ease-of-synthesis, scalability, efficiency, and fuel outputs. Given the multifaceted and interdependent properties in solar photochemistry, investigations commonly focus on a few isolated parameters and the modularity of the individual components that can eventually couple together into a working system. For example, early investigations on water splitting using *n*-type TiO_2 have heavily influenced much of the research landscape.[4] This discovery helped to motivate decades of broader efforts, such as the surface-anchoring of molecular sensitizers to TiO_2 particles, the efficacy of redox mediators, the deposition of surface cocatalyst islands, alternative preparations of TiO_2 and other types of metal-oxide particles, as well as the assembly of dye-sensitized solar cells with up to ~10−20% reported efficiencies.[5−7] However, this rapidly growing divergence and specialization in solar fuels research can also serve to hinder an understanding of the shared significance and context of current results.

Natural photosynthesis has served as a constructive paradigm and common touchstone in the overall design of a successful artificial photosynthetic approach. According to the current general understanding,[8] natural photosynthetic systems feature an antennae-like array of chlorophyll and carotenoid pigments that capture incoming visible-light photons ($\lambda \approx 400-700$ nm) to produce excited electron/hole pairs that are separated extremely quickly and efficiently. The pigment array provides downhill free-energy gradients that drive the spatial separation of electrons and holes and funnels them to separate molecular reaction centers at suitable redox potentials (e.g., CO_2 fixation and H_2O oxidation). It should be noted that the pigments outnumber the reaction centers by ~200−300:1, thereby ensuring a continuous delivery of multiple redox equivalents. The underlying and distinct elementary processes of the natural systems are, by analogy, common threads of intense research in artificial systems. In dye-sensitized solar cells for example,[9] molecular sensitizers (e.g., Ru−polypyridyl complexes) function in multiple roles, including for the absorption of solar photons, followed by the injection of excited electrons into a TiO_2 particle, and last, as the catalytic oxidation site. The spatial separation of the electrons is achieved by band bending at the TiO_2 surface as well as by any externally applied bias, before subsequently reaching a counter electrode (e.g., Pt) for the reduction half reaction. Either a facile redox couple common to both electrodes (e.g., I^-/I_3^-) can be selected for electrical energy generation or a fuel-producing set of redox couples can be chosen (e.g., H_2O/O_2 with CO_2/CH_3OH). The high degree of modularity possible makes this one of the most heavily explored solar photochemical approaches.

Many metal-oxide particles are found to be highly photocatalytically active for both oxidation and reduction reactions over their surfaces and therefore have also been heavily investigated as aqueous suspensions. A few from among hundreds of studies include particle suspensions of TiO_2,[10]

Received Date: July 15, 2010
Accepted Date: August 27, 2010
Published on Web Date: September 02, 2010

DOI: 10.1021/jz100961d | *J. Phys. Chem. Lett.* **2010**, *1*, 2719–2726

$La_2Ti_2O_7$,[11] $Sr_2Nb_2O_7$,[12] and La-doped $NaTaO_3$,[13] which can achieve quantum efficiencies within ultraviolet energies of up to ~10 to >50% for the production of H_2 and/or O_2 from aqueous solutions. Almost universally, numerous prior studies show that the surface deposition of Pt nano-islands (e.g., ~5−30 nm sizes) typically functions as a highly effective channel for the excited electrons, as shown by the orders of magnitude increase in reaction rates and the very high quantum efficiencies commonly possible. For example, an optimization of photocatalytic H_2 production over TiO_2 contained only 0.05 wt % Pt and corresponded to a surface coverage of only ~0.3%.[14] By analogy, surface cocatalysts have also been used (e.g., RuO_2, IrO_2) for assisting photocatalytic O_2 production, though typically representing the slower and overall limiting rate. While the large bandgap sizes of early transition-metal oxides (>3.0 eV) restrict their photocatalytic activities to ultraviolet wavelengths, these results have nevertheless suggested that metal-oxide particles can, under appropriate conditions, function as highly effective chromophores that can efficiently separate and drive photon-generated carriers to surface catalyst sites for enabling fuel-producing reactions. However, both high surface areas and crystallinities are critical for enhancing the charge mobility and concentration of surface reaction sites.

While the large bandgap sizes of early transition-metal oxides (>3.0 eV) restrict their photocatalytic activities to ultraviolet wavelengths, these results have nevertheless suggested that metal-oxide particles can, under appropriate conditions, function as highly effective chromophores that can efficiently separate and drive photon-generated carriers to surface catalyst sites for enabling fuel-producing reactions.

Conventional solid-state preparations of the metal oxides provide, at best, a trade-off between good crystallinity and a high surface area as a function of temperature.[15] As an alternate approach, flux synthetic conditions within molten mixtures of Na_2SO_4/K_2SO_4 or NaCl/KCl, for example, can offer enhanced metal-oxide crystallinity and homogeneity, rapid reaction times as short as under 1 h, and tunability of the particle sizes and surface areas. The first demonstration of the general utility of this approach for photocatalytic investigations was reported in the high-purity flux synthesis of La-doped $NaTaO_3$ and the (110)-layered perovskite $La_2Ti_2O_7$ photocatalysts.[16,17] Through tuning of particle sizes with platelet-shaped morphologies, the relative amounts of exposed crystallite edges and specific crystal faces were shown to be important factors in the photocatalytic activity of $La_2Ti_2O_7$ for H_2 production. Smaller $La_2Ti_2O_7$ particle sizes yield higher photocatalytic activity, as would be expected. In another example, the nanostepped surfaces of La-doped $NaTaO_3$ have been postulated as the origin of its high photocatalytic efficiency that reportedly reaches up to ~56%, as first reported by the Kudo research group.[13] Using a Na_2SO_4/K_2SO_4 flux, it was shown that lanthanum could be similarly doped into $NaTaO_3$ in controllable amounts via adding La_2O_3 into the flux media in stoichiometric concentrations. However, the modulation of dopant levels in metal oxides using flux reactions remains a relatively unexplored area. In the flux preparations, the larger particle sizes and smallest surface areas of La-doped $NaTaO_3$ unexpectedly exhibited the highest photocatalytic rates of H_2 production, thus implicating the significance of fine surface features as obtained via flux syntheses. The flux-prepared particles of both La-doped $NaTaO_3$ and $La_2Ti_2O_7$ can exhibit photocatalytic rates up to two times greater than that for the solid-state preparations. These results show that the general utility of flux-synthetic methods is in probing the expression and effect of different crystal surfaces, and which we have found represent a significant rate-limiting factor in many other metal oxides as well.

Several recently emerging band-energy strategies have been investigated for extending the range of light absorption in metal oxides out to the visible-light wavelengths.[18] In metal oxides that contain only a d^0 electron configuration, such as in TiO_2, the conduction band derives primarily from the empty 3d orbitals while the valence band originates predominantly from the filled oxygen 2p orbitals. Therefore, bandgap excitation gives rise to electrons and holes at redox potentials determined by their respective crystal orbitals. In the anatase form of TiO_2, for example, these occur at approximately −0.3 and +2.9 V (versus NHE at pH = 0), respectively.[7] Hence, a key challenge has been how to optimally lower the bandgap size while maintaining suitable redox potentials to drive photosynthetic-relevant reactions (e.g., $H_2O \rightarrow H_2 + 1/2O_2$; $CO_2 + 2H_2O \rightarrow CH_3OH + 3/2O_2$). Most approaches focus on raising the valence band energy to more closely approach the oxidation potential of water. Early transition-metal oxides that also incorporate Ag(I) or Pb(II), for example, accomplish this by combining a d^{10} or $d^{10}s^2$ electron configuration of a metal cation with the d^0 electron configuration of an early transition-metal cation. A new higher-energy valence band is formed from the filled s^2 and/or d^{10} orbitals, and that interacts with the O 2p orbitals to a varying extent. For example, $AgNbO_3$,[19] Ag_2MoO_4,[20] and $AgVO_3$,[21] all show bandgap sizes at the edge of visible-light energies, with visible-light absorption arising primarily from a metal-to-metal charge transfer between the electron-donating and electron-accepting d-orbital configurations.

Previous investigations into the solid-state preparations of $AgNbO_3$, for example, show that it has a bandgap size of ~2.75−2.81 eV and exhibits low photocatalytic rates for H_2 production in visible light using sacrificial reagents.[19,22] The preparation of $AgNbO_3$ by solid-state methods yields no

DOI: 10.1021/jz100961d | J. Phys. Chem. Lett. 2010, 1, 2719–2726

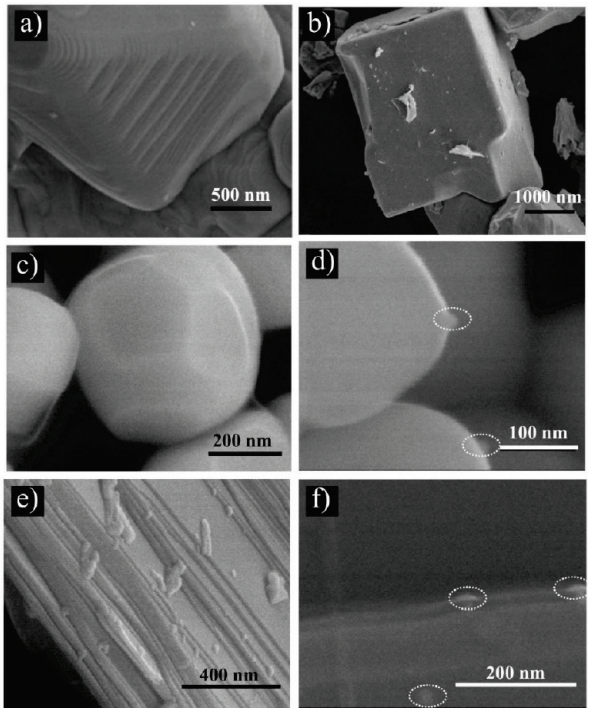

Figure 1. Field-emission SEM images of flux-prepared (a) $AgNbO_3$ using Na_2SO_4 (3:1 ratio), (b) $PbTiO_3$ using PbO (2:1 ratio), (c) $PbTiO_3$ using NaCl (20:1 ratio), (d) the same product after photodeposition of 1 wt % Pt cocatalyst, (e) $Na_2Ca_2Nb_4O_{13}$ using Na_2SO_4 (20:1 ratio), and (f) the same product after photodeposition of 1 wt % Pt cocatalyst. The Pt islands are labeled by dashed circles in (d) and (f).

well-faceted or homogeneous distribution of particle sizes and morphologies and thus does not provide a means to understand relationships between specific surface features and photocatalytic reactivity. However, the synthesis of high-crystallinity $AgNbO_3$ in a Na_2SO_4 salt flux can be used to obtain well-faceted particles with tunable size distributions from ~100 to 700 nm for short reaction times of 1 h and up to ~600−4000 nm for longer reaction times of 10 h.[22] The largest flux amounts and shortest reaction times yield the highest surface areas, and conversely, the smallest flux amounts and longest reaction times produce the smallest surface areas. Maximal visible-light photocatalytic rates for H_2 generation from aqueous methanol solutions are found for the flux-prepared $AgNbO_3$ products with the highest surface areas and smallest particle sizes. A large concentration of nanostepped terraced surfaces (~20−50 nm) was found on the majority of $AgNbO_3$ particles, as shown in Figure 1a, which were related to the highest observed photocatalytic rates. The nanostepped edges at metal-oxide surfaces create separate surface sites for the formation of H_2 and O_2, which can be demonstrated by the preferential deposition of oxidants and reductants (e.g., Ag^+, Pb^{2+}) on the step edges, such as those found in $Na_2Ca_2Nb_4O_{13}$ shown in Figure 1e and f, rare-earth-doped $NaTaO_3$, and many others.[13,16]

Another distorted-perovskite structure type with a borderline visible-light bandgap size of ~2.72−2.78 eV is $PbTiO_3$,[23] which has been previously investigated for its photocatalytic activity for overall water splitting to give O_2 and H_2 from aqueous solutions.[24] Flux synthetic techniques can be utilized to prepare $PbTiO_3$ particles in either NaCl or PbO molten fluxes at 1000 °C in just 1 h, with high purities, regular microstructures, and tunable particle sizes from ~100 to >10 000 nm.[23] These studies show that the highest surface area and smallest particle sizes of ~100−250 nm can be obtained using a NaCl flux, Figure 1c. By contrast, the use of a PbO flux results in rectangular and cube-like particles with much larger sizes of ~1000−10 000 nm, Figure 1b. Most surprisingly, the largest particle sizes and lowest surface areas exhibit the highest rates for either H_2 or O_2 formation from aqueous solutions. In analogy with the results for $AgNbO_3$, the higher photocatalytic rates were correlated with the formation of surface nanofeatures on $PbTiO_3$ particles, including readily observable edges and grooves in the samples prepared using a PbO flux. While the $PbTiO_3$ sample prepared by the solid-state method exhibited a lower surface area, it yielded higher photocatalytic rates than the NaCl flux products and rates comparable to those for the PbO flux products. The photodeposited Pt shows clustering and island formation on the solid-state sample, while the Pt is more evenly dispersed on the smoother flux-synthesized particles. Thus, surface features were shown to have a predominant effect that can reverse the typical trend of the total surface area, leading to the highest photocatalytic rates.

The two above contrasting results for $AgNbO_3$ and $PbTiO_3$ illustrate the usefulness of flux synthesis in helping to relate particle sizes, surface areas, and surface microstructures with photocatalytic activity. However, the development of more numerically-based relationships, such as for charge transfer and surface recombination rates, is prevented by the relatively broad distribution of particle features in all flux-prepared samples. For metal oxides that can be deposited electrochemically, more precisely controlled variations in particle sizes and morphologies can be achieved in order to isolate a narrower set of surfaces and formulate more exact relationships.[25] However, given the multitude of possible surfaces and surface microstructures, the knowledge of the variability of reactivity over different surfaces is a useful prerequisite for a targeted approach. A further critical direction in artificial photosynthetic research is in surface modifications and derivatizations that facilitate the desired fuel-producing reactions at the molecular level. A relatively small number of surface catalyst sites per particle would be needed to achieve an appropriate ratio of light-generated carriers to catalyst sites, similar to that found in nature and for the Pt cocatalyst islands discussed earlier. However, the optimum single-bandgap size for the most efficient use of solar radiation is ~1.4 eV,[6,7] and when added to the estimated overpotentials necessary at the catalyst sites, this increases to a debatable ~1.6−2.2 eV.

Semiconducting modifications of the early transition-metal oxides that can absorb much more deeply into the visible-light energies are needed, while also maintaining their favorable conduction band energies with respect to the H^+/H_2 and CO_2/CH_3OH redox couples. The formation of higher-energy valence bands using high concentrations of metal cation dopants was initially investigated decades ago, especially for Mn(II), Cr(III), Co(II), and Ni(II).[26,27] However, these studies revealed problematically high rates of carrier

DOI: 10.1021/jz100961d | J. Phys. Chem. Lett. 2010, 1, 2719–2726

recombination for the incompletely filled d-orbital configurations, low carrier mobility owing to the relatively isolated states, as well as photocorrosion problems in many cases. Critical determinants in overcoming these limitations are the oxidation states as well as the local and extended coordination environments of the metal cations, facts that have perhaps been too lightly considered so far. For example, reported photocorrosion problems for a particular metal oxide should not be construed as a universal indicator of the lack of photostability for a metal cation in all of its potentially expressable structures. These limitations can also find future resolution in the wide possible range of aqueous and nonaqueous solutions, surface cocatalysts and coatings, redox shuttles, and other reaction parameters, but these factors so far are typically addressed only superficially, if at all, among most of the newly explored metal oxides. Thus, it should not be commonly presumed that the initially reported photocatalytic activity of a freshly-discovered metal oxide can serve as a useful and sole assessment of its suitability toward some type of final solution in solar energy conversion, especially given the necessity of significant future research into reaction conditions, mechanisms, and particle architectures. For these reasons, the research results discussed below are more tightly focused on the attainment of the deepest possible visible-light absorption in metal oxides with suitable band energies for serving as broadly applicable sources of light-generated charge carriers for driving the fuel-producing reactions of water and/or carbon dioxide reduction. Our recent research advances have aimed at the incorporation of filled d^{10} configurations of metal cations (e.g., Ag(I) or Cu(I)) as part of the regular crystalline framework of early transition-metal oxide and oxide/organic hybrid solids, wherein the local and extended coordination geometries can both be modified.[28−30]

Thus, it should not be commonly presumed that the initially reported photocatalytic activity of a freshly-discovered metal oxide can serve as a useful and sole assessment of its suitability toward some type of final solution in solar energy conversion, especially given the necessity of significant future research into reaction conditions, mechanisms, and particle architectures.

Investigations in the copper(I) tantalate system using both solid-state and flux reactions yielded the high-purity preparations of $Cu_5Ta_{11}O_{30}$ and $Cu_3Ta_7O_{19}$.[31] In contrast to the common octahedral building blocks of perovskites, both structures contain single and double layers of edge-shared TaO_7 pentagonal bipyramids that alternate with layers of linearly coordinated Cu(I) and TaO_6 octahedra, shown in Figure 2a. Optical bandgap sizes of $Cu_5Ta_{11}O_{30}$ and $Cu_3Ta_7O_{19}$ are ∼2.59 and ∼2.47 eV, respectively. By comparison, alkali metal tantalates typically exhibit bandgap sizes in the range of ∼3.5 to >4.0 eV, such as that for $NaTaO_3$ (∼4.0 eV), which is the most efficient known UV photocatalyst. The lowest-energy bandgap transition is predicted to be indirect for both, with the highest energies of their valence bands consisting of Cu $3d^{10}$ orbitals and the lowest energies of their conduction bands consisting of Ta $5d^0$ orbitals, shown in Figure 2b. The incorporation of higher-energy $3d^{10}$ orbitals has significantly lowered the bandgap sizes of the alkali-metal tantalates by ∼1.5 eV, which thereby allows them to absorb more deeply into the visible-light energies than either Pb(II)- or Ag(I)-containing tantalates; for example, the value for $AgTaO_3$ is ∼3.4 eV.

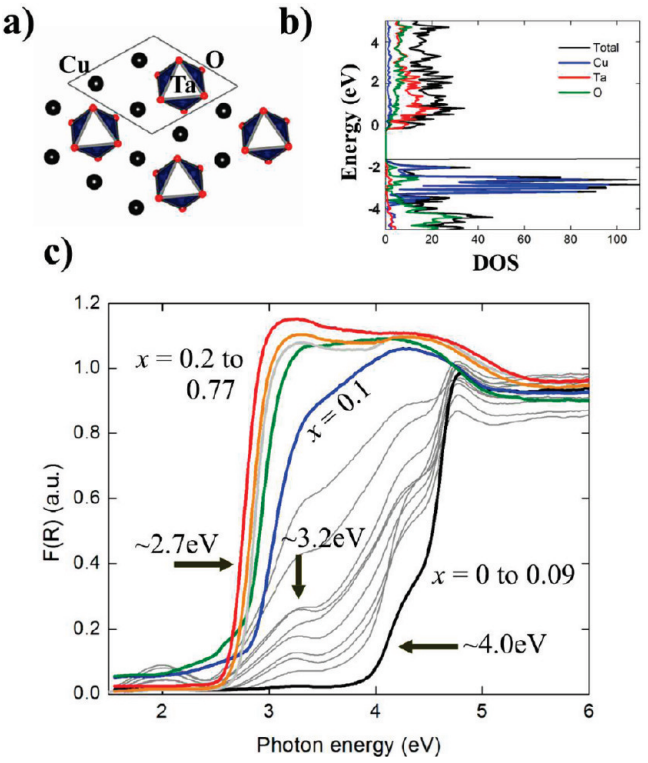

Figure 2. (a) Structural view of the Cu(I)/TaO_6 layer, (b) the calculated electronic densities-of-states for the ideal $(Cu_xNa_{1-x})_2Ta_4O_{11}$ ($x = 1$), and (c) the UV−vis diffuse reflectance spectra for the solid solution from $x = 0$ to 0.77.

A first vital feature to evaluate for the copper(I) tantalates is the redox position of their band energies resulting from the Cu $3d^{10}$ and Ta $5d^0$ orbitals with respect to the water splitting and carbon dioxide reduction half reactions. The band energies for simpler early transition-metal oxides are known to fairly accurately follow the Butler and Ginley equation based on the Mülliken electronegativities, as well as the empirically derived equation by Scaife.[27,32] However, both methods are known to typically fail in the case of metal oxides comprised of two or more transition metals. A convenient solution to this

DOI: 10.1021/jz100961d | J. Phys. Chem. Lett. 2010, 1, 2719–2726

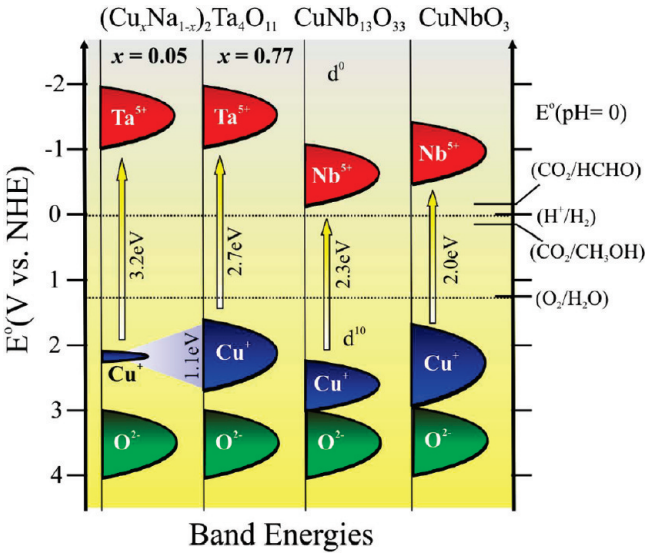

Figure 3. Calculated conduction and valence band redox potentials for the $(Cu_xNa_{1-x})_2Ta_4O_{11}$ solid solution for x = 0.05 and 0.77, $CuNb_{13}O_{33}$, and $CuNbO_3$, with the band gap transitions labeled by with arrows.

problem is found in using the $(Cu_xNa_{1-x})_2Ta_4O_{11}$ (x = 0–0.77) solid solution,[33] which has a similar structure of pentagonal bipyramidal layers, TaO_6 octahedra, and substitutionally-occupied Cu(I)/Na sites. The Scaife equation for $Na_2Ta_4O_{11}$ locates the O 2p valence band at +3.0 V and the Ta d^0 band at −1.0 V, similar to that found for $NaTaO_3$ as expected. As the Cu(I) content increases from 0 to ~77%, there is a substantial ~1.3 eV red shift of the bandgap size from ~4.0 to ~2.7 eV, shown in Figure 2c. However, at low Cu(I) concentrations (x = 0.01–0.05), a pre-edge peak appears at ~3.2 eV that corresponds to the energy of "dopant" Cu(I) $3d^{10}$ orbitals, as labeled in Figure 2. At higher concentrations, this peak broadens and grows to yield the visible-light band edge at ~2.7 eV. Thus, the Cu(I) band can be determined to be centered around ~0.8 eV higher than the O 2p valence band in this structure, at +2.2 V, before then further broadening by ~1.1 eV at x = 0.77. The resulting band energy diagram is plotted in Figure 3, which shows the conduction and valence bands to be suitably located with respect to the relevant redox couples.

While many alkali-metal niobates are reported to be highly active photocatalysts, the related Cu(I) niobates have not been well-explored yet owing to the difficulties in their high-purity preparation and structural characterization. Current results in this system show that $CuNbO_3$, $CuNb_3O_8$, and $CuNb_{13}O_{33}$ can all be readily synthesized using either excess Cu_2O or a CuCl flux (unpublished results). Small visible-light bandgap sizes of only ~1.95, ~1.45, and ~2.25 eV are obtained for each, respectively, shown in Figure 4c. The comparable alkali metal compositions, for example, $NaNbO_3$, $NaNb_3O_8$, and $NaNb_{13}O_{33}$, exhibit UV bandgap sizes of ~3.4, ~3.6, and ~3.1 eV, respectively. As found for the copper(I) tantalates, the reduction of bandgap size arises from a new higher-energy valence band originating primarily from the Cu $3d^{10}$ orbitals mixed with O 2p orbitals, Figure 4a and b. Favorably, $CuNb_{13}O_{33}$ forms a solid solution with $NaNb_{13}O_{33}$, that is, as in

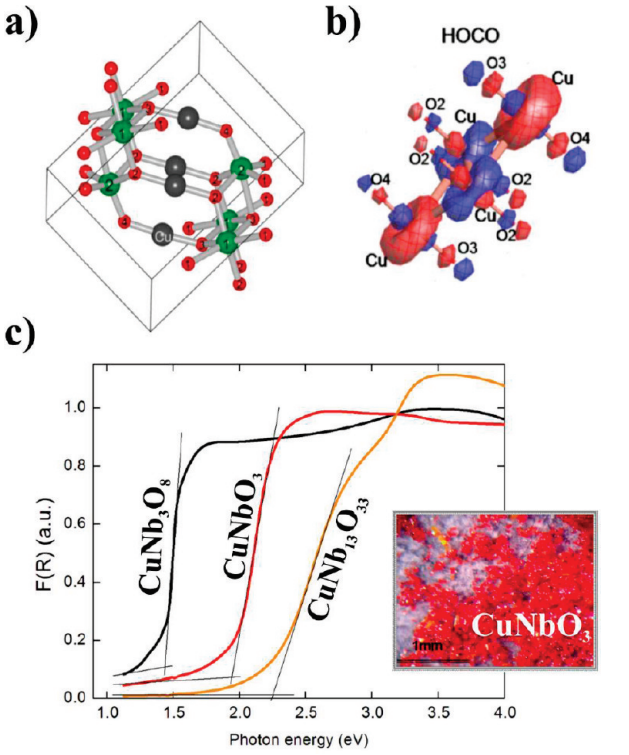

Figure 4. (a) Structural view of $CuNbO_3$ (gray atoms = Cu; red atoms = O; green atoms = Nb) with the unit cell drawn, (b) one of the crystal orbitals of its highest occupied valence levels, and (c) the UV–vis diffuse reflectance spectra of the three copper(I) niobates (labeled), inset with an optical picture of the reddish-colored $CuNbO_3$ product.

$Cu_xNa_{1-x}Nb_{13}O_{33}$, which demonstrates a substantial ~0.8 eV red shift of the bandgap size across the series. Following the same approach as that described for the $(Cu_xNa_{1-x})_2Ta_4O_{11}$ solid solution, these results can be used to approximately locate the position of the new Cu $3d^{10}$ band energy on a redox scale, shown in Figure 3. The decreasing bandgap size across this series correlates well with the increasing amount of Cu(I), owing to the increasing valence band dispersion, and is consistent with the electronic structure calculations. Also, the Nb d-band tracks upward in energy to a smaller extent across the series of copper(I) niobates, which is shown in Figure 3 for $CuNbO_3$. While the redox potentials for water splitting and carbon dioxide reduction have been more closely bracketed, a further fine-tuning of the band positions to specific energies will require future planned electrochemical measurements as well as a more accurate knowledge of other key parameters, such as the required surface overpotentials for the reactions.

Early demonstrations of the impressive photocatalytic efficiencies for the ultraviolet irradiation of suspended metal-oxide particles in aqueous solutions have perhaps served to distort and overemphasize their potential for stand-alone use with the full solar spectrum. Testament to this are the numerous studies that have aimed to extend the range of metal-oxide photocatalysts to the visible-light energies, but that have so far continually failed to produce the same level of success. The described research efforts on the

DOI: 10.1021/jz100961d | J. Phys. Chem. Lett. 2010, 1, 2719–2726

flux synthesis of La-doped $NaTaO_3$, $La_2Ti_2O_7$, $AgNbO_3$, and $PbTiO_3$ show that their photocatalytic activities are not solely the function of surface area but are determined to a large extent by the surface features that aid in charge transfer and/or electron−hole separation. Deeper analyses of the factors governing charge-transfer and recombination rates across other photocatalytic systems have previously led to similar conclusions regarding the surface-mediated control of photoelectrode-based energy conversion schemes.[34] Further evidence of this is found in the commonly observed preferential photodeposition of cocatalysts such as Pt or RuO_2 over specific surface features, and while boosting the activity by factors of hundreds or more, is also an intriguing signature of the underlying pathways of charge migration and separation.[10,14] A natural conclusion is that while many types of early transition-metal oxide particles can both efficiently absorb ultraviolet photons and separate the generated electron−hole pairs, the resulting photocatalytic rates may or may not be reflective of this property, depending on the surfaces and reactions involved. This limitation should be substantially more pronounced in the case of semiconducting oxides, where a closer approach to the redox potentials necessarily results in much smaller overpotentials and interfacial electric fields at the surfaces. Thus, the current lack of success in achieving high visible-light-driven photocatalytic activities for metal oxides may quite often reflect these limitations, assuming that the thermodynamics are appropriate, making the use of more finely-tuned surface features and reaction centers nearly mandatory.

Early demonstrations of the impressive photocatalytic efficiencies for the ultraviolet irradiation of suspended metal-oxide particles in aqueous solutions have perhaps served to distort and overemphasize their potential for stand-alone use with the full solar spectrum.

While the flux-synthetic technique facilitates a general tunability of particle sizes and surface areas, this does not currently provide a route to a finer molecular-level control over surface features. Examples of surface-deposited core−shell cocatalysts, such as in $M@Cr_2O_3$ (M = Rh, Ir, Pt) reported first by the Domen research group,[35] seem to show much promise in this direction as compared to the simpler Pt or RuO_2 islands. However, a deeper understanding and investigation of these reactions should now be possible by surface attachments to molecular catalysts, such as the "blue dimer" $[(bpy)_2(H_2O)RuORu(H_2O)(bpy)_2]^{4+}$ complex[36] or the bioinspired Mn-oxo clusters.[37] The paradigm of natural photosynthesis supports the sagacity of the latter approach,

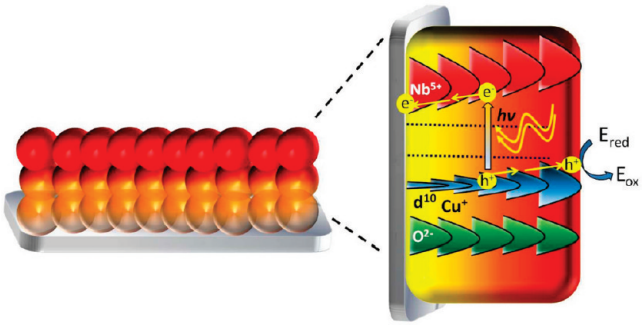

Figure 5. Multilayered gradient of metal oxides containing increasing Cu(I) content vertically (left) and a schematic of the resulting opposing energy gradients for electrons and holes (right).

wherein the array of light-harvesting chromophores is used to achieve efficient spatial separation and funneling of the excited electrons and holes to the molecular reaction centers. In regards to carrier mobility, several metal oxides containing linearly-coordinated Cu(I) are currently under investigation for their relatively high p-type conductivity, including $CuAlO_2$,[38] $CuScO_2$, and related delafossite structures.[39] Their p-type transport properties are attributed to the Cu−O covalency and to the high hole concentrations possible via extrinsic and/or intrinsic types of defects, that is, acceptor dopant cations and interstitial O, respectively. By analogy, nearly all of the examples presented herein contain linearly-coordinated Cu(I) and a high concentration of potential defect sites via underoccupancy of the Cu(I) sites, such as in $Cu_5Ta_{11}O_{30}$ (Cu sites 17% vacant) and $(Cu_xNa_{1-x})_2Ta_4O_{11}$ (Cu sites 33% vacant). This high concentration of unfilled sites can provide convenient access for extrinsic and intrinsic p/n-types of defects, which is part of ongoing research. Further, their solid solution forms, as in $(Cu_xNa_{1-x})_2Ta_4O_{11}$ and $Cu_xNa_{1-x}Nb_{13}O_{33}$, highlight a particularly intriguing route to achieve charge separation through either multilayered or continuous composition gradients, such as shown in Figure 5. Opposing free-energy gradients for both electrons and holes can be conveniently exploited in these cases where both the conduction and valence energy bands are known to track each other in energy with increasing Cu(I) content.

Nature, it seems, has capitalized on foreign-component integration to make dramatic evolutionary jumps, such as in the example of green plant cells that assimilated light-harvesting chloroplasts from an endosymbiotic relationship with cyanobacterium. Cyanobacterium, in turn, is thought to have itself assembled the oxygen-evolving Mn_4 complex from structurally-related inorganic components found in minerals like hollandite.[40] If analogous revolutionary strides are to be realized in artificial photosynthesis, then future research must be aimed toward the more diverse integration of synergistically functioning chemical architectures. As a step in this direction, the new copper(I) niobate and copper(I) tantalate semiconductors show a broadly applicable foundation for the absorption of solar energy with band energies that bracket important fuel-generating redox couples. Further, these semiconducting oxides can be expressed in many configurations, such as in multilayered, mesoporous, and core−shell formats,

DOI: 10.1021/jz100961d | J. Phys. Chem. Lett. 2010, 1, 2719–2726

which are currently under investigation for use in enhancing charge separation and surface areas. These results and current investigations will hopefully provide new convergent roads to the future incorporation of incident photons into many of the redox catalysts currently studied only electrochemically at present.

AUTHOR INFORMATION

Corresponding Author:

*To whom correspondence should be addressed. E-mail: Paul_Maggard@ncsu.edu. Tel. 1-919-515-3616.

Biographies

Upendra A. Joshi received his Ph.D. in Chemical Engineering from Pohang University of Science and Technology, Republic of South Korea, in 2006 and, following a one-year period as postdoctoral fellow, moved to the University of Liverpool, U.K., for postdoctoral research (2008−2010). Currently, he is working on a photoelectrochemical cell system and photocatalysis research at North Carolina State University with Prof. Paul Maggard as a postdoctoral research associate. His other interests include hydrothermal synthesis of nanomaterials and heterogeneous catalysis.

Andriy Palasyuk received his Ph.D. in Inorganic Chemistry at Ivan Franko National University of Lviv, Ukraine, in 2002, followed subsequently by postdoctoral research with Prof. Dr. Gerd Meyer at University of Cologne, Germany (2003−2006), Prof. John Corbett at Iowa State University/Ames Laboratory, DOE (2006−2008), and Prof. Paul Maggard at North Carolina State University (2008−present). His research interests include the structural chemistry of inorganic materials (intermetallics, oxides, etc.), their physical properties, as well as theoretical computations of electronic structures.

David Arney received his Bachelor's Degree in Physics and Chemistry from Hampden-Sydney College in 2005. He is currently a senior graduate student under the direction of Prof. Paul Maggard at North Carolina State University and is working on the synthesis and properties of heterometallic oxides as novel photocatalysts for water splitting reactions.

Paul A. Maggard received his Ph.D. from Iowa State University in 2000. He then worked 2 years at Northwestern University as a postdoctoral associate in 2000−2002 before joining the chemistry faculty at North Carolina State University in 2002, where he is currently Associate Professor of chemistry. His current research efforts involve the flux and hydrothermal synthesis of heterometallic transition-metal oxides and oxide/organic hybrids and investigation of their optical, photocatalytic, and magnetic properties. More information can be found at his website: http://www4.ncsu.edu/~pamaggar/.

ACKNOWLEDGMENT The authors acknowledge support of this research from the Chemical Sciences, Geosciences and Biosciences Division, Office of Basic Energy Sciences, Office of Science, U.S. Department of Energy (DE-FG02-07ER15914).

REFERENCES

(1) Osterloh, F. E. Inorganic Materials as Catalysts for Photochemical Splitting of Water. *Chem. Mater.* **2008,** *20*, 35–54.

(2) Halmann, M. Photoelectrochemical Reduction of Aqueous Carbon Dioxide on *p*-Type Gallium Phosphide in Liquid Junction Solar Cells. *Nature* **1978,** *275*, 115–116.

(3) Hoffmann, M. R.; Martin, S. T.; Choi, W.; Bahnemann, D. F. Environmental Applications of Semiconductor Photocatalysis. *Chem. Rev.* **1995,** *95*, 69–96.

(4) Fujishima, A.; Honda, K. Electrochemical Photolysis of Water at a Semiconductor Electrode. *Nature* **1972,** *238*, 37–38.

(5) Grätzel, M. Photoelectrochemical Cells. *Nature* **2001,** *414*, 338–344.

(6) Tan, M. X.; Laibinis, P. E.; Nguyen, S. T.; Kesselman, J. M.; Stanton, C. E.; Lewis, N. S. Principles and Applications of Semiconductor Photoelectrochemistry. *Prog. Inorg. Chem.* **1994,** *41*, 41–144.

(7) Archer, M. D.; Nozik, A. J. *Nanostructured and Photoelectrochemical Systems for Solar Photon Conversion*; Imperial College Press: London, U.K., 2008; Vol. 3.

(8) Vassiliev, S.; Bruce, D. Toward Understanding Molecular Mechanisms of Light Harvesting and Charge Separation in Photosystem II. *Photosynth. Res.* **2008,** *97*, 75–89.

(9) O'Regan, B.; Grätzel, M. A Low-Cost, High-Efficiency Solar Cell Based on Dye-Sensitized Colloidal TiO_2 Films. *Nature* **1991,** *353*, 737–740.

(10) Yamaguti, K.; Sato, S. Photolysis of Water over Metallized Powdered Titanium Dioxide. *J. Chem. Soc., Faraday Trans. 1* **1985,** *81*, 1237–1246.

(11) Kim, H. G.; Hwang, D. W.; Bae, S. W.; Jung, J. H.; Lee, J. S. Photocatalytic Water Splitting Over $La_2Ti_2O_7$ Synthesized by the Polymerizable Complex Method. *Catal. Lett.* **2003,** *91*, 193–198.

(12) Kudo, A.; Kato, H.; Nakagawa, S. Water Splitting Into H_2 and O_2 on New $Sr_2M_2O_7$ (M = Nb and Ta) Photocatalysts with Layered Perovskite Structures: Factors Affecting the Photocatalytic Activity. *J. Phys. Chem. B* **2000,** *104*, 571–575.

(13) Kato, H.; Asakura, K.; Kudo, A. Highly Efficient Water Splitting Into H_2 and O_2 Over Lanthanum-Doped $NaTaO_3$ Photocatalysts with High Crystallinity and Surface Nanostructure. *J. Am. Chem. Soc.* **2003,** *125*, 3082–3089.

(14) Kiwi, J.; Grätzel, M. Optimization of Conditions for Photochemical Water Cleavage. Aqueous Pt/TiO_2 (Anatase) Dispersions under Ultraviolet Light. *J. Phys. Chem.* **1984,** *88*, 1302–1307.

(15) Tanaka, K.; Capule, M. F. V.; Hisanaga, T. Effect of Crystallinity of TiO_2 on Its Photocatalytic Action. *Chem. Phys. Lett.* **1991,** *187*, 73–76.

(16) Porob, D.; Maggard, P. A. Flux Syntheses of La-doped $NaTaO_3$ and Its Photocatalytic Activity. *J. Solid State Chem.* **2006,** *179*, 1727–1732.

(17) Arney, D.; Porter, B.; Greve, B.; Maggard, P. A. New Molten-Salt Synthesis and Photocatalytic Properties of $La_2Ti_2O_7$ Particles. *J. Photochem. Photobiol. A: Chem.* **2008,** *199*, 230–235.

(18) Inoue, Y. Photocatalytic Water Splitting by RuO_2-Loaded Metal Oxides and Nitrides with d^0- and d^{10}-Related Electronic Configurations. *Energy Environ. Sci.* **2009,** *2*, 364–386.

(19) Kato, H.; Kobayashi, H.; Kudo, A. Role of Ag^+ in the Band Structures and Photocatalytic Properties of $AgMO_3$ (M: Ta and Nb) with the perovskite structure. *J. Phys. Chem. B* **2002,** *106*, 12441–12447.

(20) Kato, H.; Matsudo, N.; Kudo, A. Photophysical and Photocatalytic Properties of Molybdates and Tungstates with a Scheelite Structure. *Chem. Lett.* **2004,** *33*, 1216–1217.

(21) Konta, R.; Kato, H.; Kobayashi, H.; Kudo, A. Photophysical Properties and Photocatalytic Activities Under Visible Light Irradiation of Silver Vanadates. *Phys. Chem. Chem. Phys.* **2003,** *5*, 3061–3065.

(22) Arney, D.; Hardy, C.; Greve, B.; Maggard, P. A. Flux Synthesis of $AgNbO_3$: Effect of Particle Surfaces and Sizes on Photocatalytic Activity. *J. Photochem. Photobiol. A: Chem.* **2010,** *214*, 54–60.

(23) Arney, D.; Watkins T.; Maggard, P. A. Effects of Particle Sizes and Surface Features on Photocatalytic H_2/O_2 Production Using $PbTiO_3$. *J. Am. Ceram. Soc.* **2010**, Submitted.
(24) Kim, H. G.; Becker, O. S.; Jang, J. S.; Ji, S. M.; Borse, P. H.; Lee, J. S. A Generic Method of Visible-Light Sensitization for Perovskite-Related Layered Oxides: Substitution Effect of Lead. *J. Solid State Chem.* **2006,** *179*, 1214–1218.
(25) Choi, K. S. Shape Effect and Shape Control of Polycrystalline Semiconductor Electrodes for Use in Photoelectrochemical Cells. *J. Phys. Chem. Lett.* **2010,** *1*, 2244–2250.
(26) Rauh, R. D.; Buzby, J. M.; Reise, T. F.; Alkaitis, S. A. Design and Evaluation of New Oxide Photoanodes for the Photoelectrolysis of Water with Solar Energy. *J. Phys. Chem.* **1979,** *83*, 2221–2226.
(27) Scaife, D. E. Oxide Semiconductors in Photoelectrochemical Conversion of Solar Energy. *Solar Energy* **1980,** *25*, 41–54.
(28) Lin, H.; Maggard, P. A. Copper(I)−Rhenate Hybrids: Syntheses, Structures, and Optical Properties. *Inorg. Chem.* **2006,** *46*, 1283–1290.
(29) Lin, H.; Maggard, P. A. Ligand-Mediated Interconversion of Multiply-Interpenetrating Frameworks in Cu(I)/Re(VII)-Oxide Hybrids. *Inorg. Chem.* **2009,** *48*, 8940–8946.
(30) Lin, H.; Maggard, P. A. Microporosity, Optical Bandgap Sizes, and Photocatalytic Activity of M(I)−Nb(V) (M = Cu, Ag) Oxyfluoride Hybrids. *Cryst. Grow. Des.* **2010,** *10*, 1323–1331.
(31) Palasyuk, O.; Palasyuk, A.; Maggard, P. A. Syntheses, Optical Properties and Electronic Structures of Copper(I) Tantalates: $Cu_5Ta_{11}O_{30}$ and $Cu_3Ta_7O_{19}$. *J. Solid State Chem.* **2010,** *183*, 814–822.
(32) Butler, M. A.; Ginley, D. S. Prediction of Flatband Potentials at Semiconductor-Electrolyte Interfaces from Atomic Electronegativities. *J. Electrochem. Soc.* **1978,** *125*, 228–232.
(33) Palasyuk, O.; Palasyuk, A.; Maggard, P. A. Site-Differentiated Solid Solution in $(Na_{1-x}Cu_x)_2Ta_4O_{11}$ and its Electronic Structure and Optical Properties. *Inorg. Chem.* **2010**, Submitted.
(34) Lewis, N. S. Chemical Control of Charge Transfer and Recombination at Semiconductor Photoelectrode Surfaces. *Inorg. Chem.* **2005,** *44*, 6900–6911.
(35) Maeda, K.; Teramura, K.; Lu, D.; Saito, N.; Inoue, Y.; Domen, K. Noble-Metal/Cr_2O_3 Core/Shell Nanoparticles for Photocatalytic Overall Water Splitting. *Angew. Chem., Int. Ed.* **2006,** *45*, 7806–7809.
(36) Gersten, S. W.; Samuels, G. J.; Meyer, T. J. Catalytic Oxidation of Water by an Oxo-Bridged Ruthenium Dimer. *J. Am. Chem. Soc.* **1982,** *104*, 4029–4030.
(37) Brimblecombe, R.; Dismukes, G. C.; Swiegers, G. F.; Spiccia, L. Molecular Water Oxidation Catalysts for Photoelectrochemical Cells. *Dalton Trans.* **2009,** 9374–9384.
(38) Kawazoe, H.; Yasukawa, M.; Hyodo, H.; Kurita, M.; Yanagi, H.; Hosono, H. P-Type Electrical Conduction in Transparent Thin Films of $CuAlO_2$. *Nature* **1997,** *389*, 939–942.
(39) Ingram, B. J.; Harder, B. J.; Hrabe, N. W.; Mason, T. O.; Poeppelmeier, K. R. Transport and Defect Mechanisms in Cuprous Delafossites. 2. $CuScO_2$ and $CuYO_2$. *Chem. Mater.* **2004,** *16*, 5623–5629.
(40) Sauer, K.; Yachandra, V. K. A Possible Evolutionary Origin for the Mn_4 Cluster of the Photosynthetic Water Oxidation Complex from Natural MnO_2 Precipitates in the Early Ocean. *Proc. Natl. Acad. Sci. U.S.A.* **2002,** *99*, 8631–8636.

DOI: 10.1021/jz100961d | *J. Phys. Chem. Lett.* **2010,** *1*, 2719–2726